2017

PET study of sphingosine-1-phosphate receptor 1 expression in response to vascular inflammation in a rat model of carotid injury

Hui Liu
Washington University School of Medicine in St. Louis

Hongjun Jin
Washington University School of Medicine in St. Louis

Xuyi Yue
Washington University School of Medicine in St. Louis

Junbin Han
Washington University School of Medicine in St. Louis

Pamela Baum
Washington University School of Medicine in St. Louis

See next page for additional authors

Molecular Imaging
Volume 16 : 1-7
© The Author(s) 2017
Reprints and permission:
sagepub.com/journalsPermissions.nav
DOI: 10.1177/1536012116689770
journals.sagepub.com/home/mix
SAGE

PET Study of Sphingosine-1-Phosphate Receptor 1 Expression in Response to Vascular Inflammation in a Rat Model of Carotid Injury

Hui Liu, PhD, MD[1], Hongjun Jin, PhD[1], Xuyi Yue, PhD[1], Junbin Han, PhD[1], Pamela Baum, SRS[2], Dana R. Abendschein, PhD[2], and Zhude Tu, PhD[1]

Abstract

Sphingosine-1-phosphate receptor (S1PR) activation plays a key role in vascular inflammatory response. Here, we report in vivo validation of [^{11}C]TZ3321, a potent S1PR1 radioligand, for imaging vascular inflammation in a rat model of carotid injury. The right common carotid artery of male adult Sprague-Dawley rats was injured by balloon overinflation that denuded the endothelium and distended the vessel wall. Animals received a 60-minute micro-positron emission tomography (micro PET) scan with [^{11}C]TZ3321 at 72 hours after injury. Ex vivo autoradiography was also conducted. The expression and cellular location of S1PR1 were examined by immunohistological analysis. Three-dimensional (3D) reconstruction of the first 100-second microPET/computed tomography (CT) image indicated the location of bilateral common carotid arteries. [^{11}C]TZ3321 displayed significantly higher accumulation (standardized uptake values: 0.93 ± 0.07 vs 0.78 ± 0.09, $n = 6$, $P = .001$) in the injured carotid artery than in the contralateral side. Increased tracer uptake in the injured artery was confirmed by autoradiography (photostimulated luminescence measures: 85.5 ± 0.93 vs 71.48 ± 6.22, $n = 2$). Concordantly, high S1PR1expression was observed in infiltrated inflammatory cells in the injured artery. Our studies demonstrate [^{11}C]TZ3321 microPET is able to detect the acute upregulation of S1PR1 expression in inflamed carotid artery. Therefore, [^{11}C]TZ3321 has potential to be a PET radiotracer for detecting early inflammatory response and monitoring therapeutic efficacy of vascular inflammation.

Keywords

sphingosine-1-phosphate receptor 1, vascular inflammation, radioligand, PET

Introduction

Recent therapeutic advances have led to a decrease in cardiovascular morbidity and mortality. Despite this reduction, vascular disease remains a global health concern with associated costs. Positron emission tomography (PET) imaging, which can noninvasively quantify in vivo pathological processes occurring within the arterial system, could be used for early diagnosis and monitoring therapeutic effects. Currently, [^{18}F]-Fludeoxyglucose (FDG) is the most commonly used PET tracer in vascular imaging. However, FDG-PET highlights all regions of high-glucose metabolism but lacks target specificity, which is the major shortcoming.[1] To overcome this limitation, ligands for specific targets involved in vascular pathologies have been developed and radiolabeled for PET imaging.

Sphingosine-1-phosphate (S1P), which binds to 5 G protein–coupled receptors (S1PR1 to S1PR5), is a bioactive lipid with key functions in the immune, inflammatory, and cardiovascular systems.[2] In particular, S1PR1 is expressed in endothelial cells and vascular smooth muscle cells (VSMCs), as well as in most leucocytes.[2] The activation and/or upregulation of S1PR1 are involved in various vascular pathologies,[3,4] including atherosclerosis and restenosis, a major cause of morbidity in both developed and developing countries. Thus,

[1] Department of Radiology, Washington University School of Medicine, St Louis, MO, USA
[2] Center for Cardiovascular Research, Department of Internal Medicine, Washington University School of Medicine, St Louis, MO, USA

Submitted: 19/08/2016. Revised: 10/12/2016. Accepted: 15/12/2016.

Corresponding Author:
Zhude Tu, Department of Radiology, Washington University School of Medicine, St Louis, MO 63110, USA.
Email: tuz@mir.wustl.edu

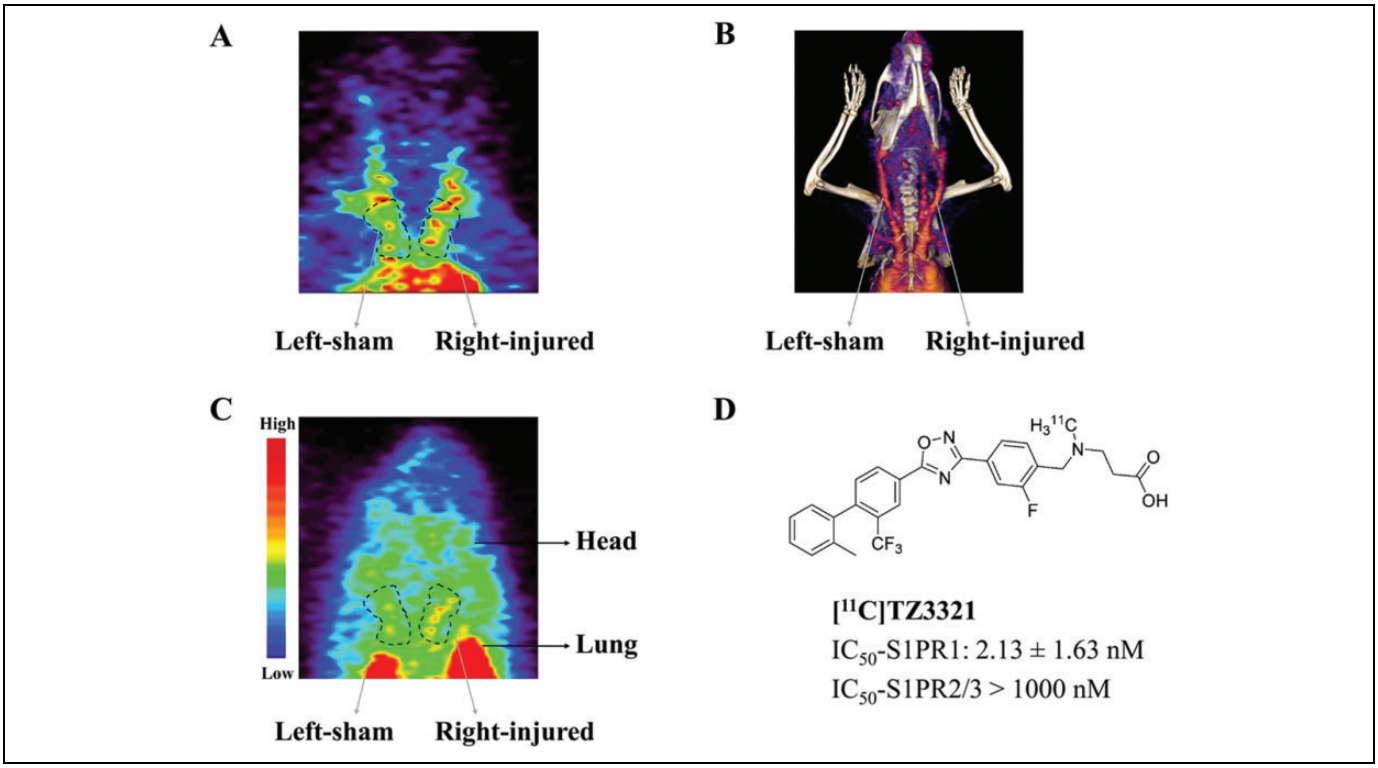

Figure 1. The representative micro-positron emission tomography (micro PET) images of balloon injured rat carotid artery using a potent sphingosine-1-phosphate receptor 1 (S1PR1) PET radiotracer [^{11}C]TZ3321. MicroPET image (A, two-dimensional[2D] image) and coregistered PET/computed tomography [CT] image of the first 100-second scan (B, three-dimensional (3D) image) indicated the blood perfusion in bilateral carotid arteries and were used to locate bilateral common carotid arteries. MicroPET image (C, 2D image) of the totally 60-minute scan showed higher tracer uptake in the injured carotid artery area than the sham side. D, the molecular structure of [^{11}C]TZ3321.

S1PR1 provides a potential target for both therapeutic and in vivo imaging purposes.

Investigations of arterial response to mechanical injury offer potential clues for human atherosclerosis etiology and restenosis.[5] The rat carotid artery balloon injury model is a well-established animal model that utilizes mechanical damage caused by a balloon catheter and results in mural distension and the removal of the endothelial lining. Endothelial denudation leads to an acute inflammatory response, the activation and deposition of platelets with recruitment of circulating leucocytes, followed by the adaptive response, including VSMC proliferation, migration, and the establishment of an invasive neointima.[6] In line with the acute inflammatory response, the S1PR1 messenger RNA level of the injured artery is dramatically increased at 72 hours postinjury.[3] Therefore, in vivo measurement of S1PR1, via a S1PR1-specific radiolabeled PET tracer, could be useful for monitoring vascular inflammation.

We previously reported the synthesis and radiolabeling of a potent S1PR1 ligand TZ3321 (3-((2-fluoro-4-(5-(2′-methyl-2-(trifluoromethyl)-[1,1′-biphenyl]-4-yl)-1,2,4-oxadiazol-3-yl)benzyl)methyl)amino)-propanoic acid, Figure 1D), which shows high in vitro binding potency (Half maximal inhibitory concentration $IC_{50} = 2.13 \pm 1.63$ nM) and selectivity toward S1PR1 (IC_{50} values >1000 nM for S1PR2 and S1PR3).[7] The radioligand [^{11}C]TZ3321 has been successfully utilized to detect in vivo inflammatory conditions by microPET scan in 2 different rodent models.[7,8] The aim of the current study is to investigate the possibility of assessing the change of S1PR1 levels in the arterial wall during acute vascular inflammation using [^{11}C]TZ3321 PET.

Materials and Methods

Radiosynthesis

The radioligand [^{11}C]TZ3321 was produced as reported recently by our group.[7] The radioactive product was obtained with radiochemistry yield of 60 ± 10% (n > 10, decay corrected to the end of bombardment [EOB]); specific activity of 152 - 575 GBq/μmol (n > 10, decay corrected to EOB); and chemical purity and radiochemical purity >98% (n > 10).

Rat Carotid Artery Balloon Injury Model

All animal experiments were conducted in compliance with the Guidelines for the Care and Use of Research Animals under protocols approved by Washington University's Animal Studies Committee. Mature, male Sprague-Dawley (SD) rats (Charles River Laboratories, Inc, Wilmington, Massachusetts) were used for all experiments.

The rat carotid artery balloon injury procedure was carried out according to published methods.[9] Briefly, 350 to 700 g male SD rats were anesthetized with isoflurane (1-3%). The

trifurcation of the right common carotid artery with the external and internal carotid branches was exposed by a ventral skin incision and blunt dissection. Sterile sutures were placed around the common and external carotid artery (ECA) branch in order to isolate the ECA branch for vascular access and to control blood flow. A deflated sterile balloon catheter (2F Fogarty, Edwards Lifesciences, Irvine, California) was introduced through an arteriotomy in the external branch and passed proximally down the common carotid into the aorta. Slight inflation of the balloon with saline and withdrawal of the catheter identified when it began to engage the brachiocephalic artery. The balloon pressure was then decreased just enough to allow the withdrawal of the catheter with rotation along the full length of the common carotid artery to the area of the carotid trifurcation. The balloon was then deflated, and this procedure was repeated 3 times. The arteriotomy was closed proximally, and blood flow through the common carotid artery was restored. The contralateral (left) common carotid artery and branches were similarly exposed without ligation or catheterization as a sham control.

MicroPET Imaging and Data Process

Small-animal microPET imaging was performed at ~72 hours following carotid injury on an Inveon PET/CT system (Siemens Inc, Knoxville, Tennessee). Positron emission tomography scans were conducted under light anesthesia (~2% isoflurane) delivered by a nose cone. The rats were secured using a custom-designed acrylic restraining device, with their head and neck inside the field of the window of the Inveon PET/CT system. Following a transmission scan and a computed tomography (CT) for anatomical coregistration, animals received a bolus intravenous (IV) injection of [^{11}C]TZ3321 (19-37 MBq). A list-mode protocol was used with 60-minute dynamic data acquisition.

Image reconstructions were performed and analyzed using microPET Manager 2.3.3.6, ASIPro 6.3.3.0 (Siemens Inc) and Inveon Research Workstation built-in software IRW 4.2 program (Siemens Inc). The list-mode data of the emission scans were reframed into a dynamic sequence of 1 × 3 s, 6 × 2 s, 9 × 5 s, 6 × 10 s, 4 × 30 s, 2 × 60 s, 2 × 2 min, 10 × 5 min frames. The data were reconstructed per time frame using an iterative reconstruction algorithm and corrected for decay, random coincidences, scatter, and attenuation. Regions of interest (ROIs) were drawn over the summary of the first 100-second images, which indicated the blood perfusion in bilateral carotid arteries. Time-activity curves (TACs) were obtained and were expressed as dimensionless standardized uptake values (SUVs). The parameter SUV is defined as (tissue activity concentration [MBq/g] × body weight (g)/injected dose [MBq]). Two-tailed paired *t* test was used for the comparison of the tracer uptake in bilateral carotid arteries. A *P* value less than .05 was considered statistically significant.

Ex Vivo Autoradiography

Ex vivo autoradiography was performed at ~72 hours following the carotid injury. Rats were euthanized at 30 minutes following a bolus injection of [^{11}C]TZ3321 (74-110 MBq). Bilateral common carotid arteries were then dissected and cut in half. One half of the artery was fixed in 10% formalin and processed for histological and immunohistochemical examination. The other half was exposed immediately to a BAS storage phosphor screen (BAS-IP-MS-2025) in an imaging cassette for 2 hours at −80°C. The distribution of radioactivity was visualized by a Fuji Bio-Imaging Analyzer FLA-7000 (Fuji Film, Tokyo, Japan). Photostimulated luminescence was quantified using Multi Gauge v3.0 software. Data were background corrected and expressed as photostimulated luminescence signals per square millimeter (PSL/mm^2).

Histological and Immunological Analysis

Carotid artery samples were fixed in 10% formalin, then embedded in paraffin and cut into 5 μm sections. Hematoxylin and eosin (H&E) staining was performed to visualize lesion morphology of carotid arteries. For immunohistochemical analysis of S1PR1 expression, sections were deparaffinized in xylene and rehydrated through a graded alcohol series to water. Endogenous peroxidase activity was quenched with 3% H_2O_2 in methanol for 5 minutes. Slides were incubated in blocking buffer for 30 minutes before the incubation with a 1:50 dilution of a rabbit anti-rat S1PR1 antibody (Santa Cruz biotechnology, Santa Cruz, California) overnight at 4°C. The primary antibody binding was detected using an anti-rabbit horseradish peroxidase-3,3′-diaminobenzidine (HRP-DAB) staining kit (R&D Systems, Minneapolis, Minnesota) according to the manufacturer's instructions. To further identify cell types expressing S1PR1 receptor, immunofluorescence was performed. Sections were incubated in blocking buffer for 60 minutes following deparaffinization, rehydration, and endogenous peroxidase deactivation. The primary antibodies were added as a mixture (rabbit anti-rat S1PR1 [1:50] and mouse anti-rat Cluster of Differentiation 68 (CD68) [1:100, Abcam, Cambridge, Massachusetts]/CD3 [1:50, Santa Cruz biotechnology]/HIS48 [1:50, Santa Cruz biotechnology] antibodies) and incubated with the slides at 4°C overnight. The secondary fluorescently labeled antibodies (fluorescein-conjugated goat anti-mouse immunoglobulin G (IgG) antibody [1:100, Jackson ImmunoResearch Lab, West Grove, Pennsylvania] and rhodamine-conjugated donkey anti-rabbit IgG antibody [1:100, Jackson ImmunoResearch Lab]) were added and incubated in the dark for 60 minutes. A Nikon E600 (Nikon Instruments Inc., Melville, New York) microscope coupled with a charge-coupled device camera was used to obtain all photomicrographs.

Results

MicroPET Studies

The summary of the first 100-second microPET scan images (Figure 1A) and 3D reconstruction of microPET/CT scans in the same period (Figure 1B), which indicated the blood perfusion in bilateral carotid arteries, successfully located

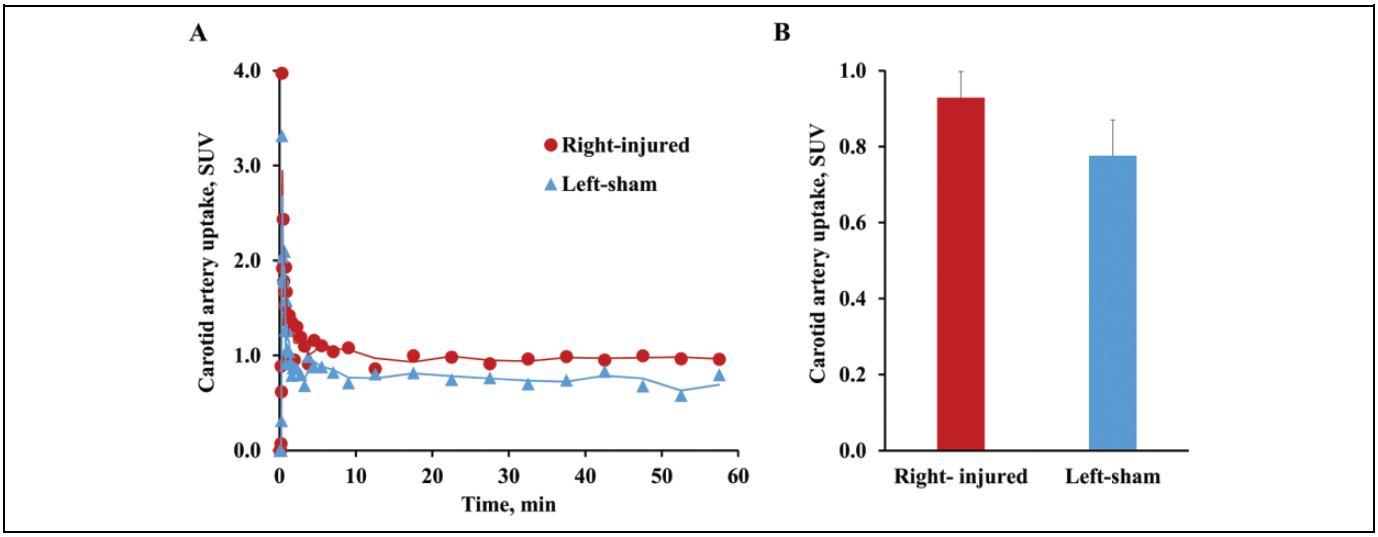

Figure 2. Tissue Time-activity curves (TACs) of [^{11}C]TZ3321 uptake in balloon injured rat carotid artery. Both the representative TACs (A) and the quantification of tracer uptake in 15 to 50-minute postinjection (B) revealed a 19.6% increase (standardized uptake values: 0.93 $\pm$ 0.07 vs 0.78 $\pm$ 0.09, n = 6, P = .001) of standardized uptake value (SUV) at 72 hours following the balloon injury.

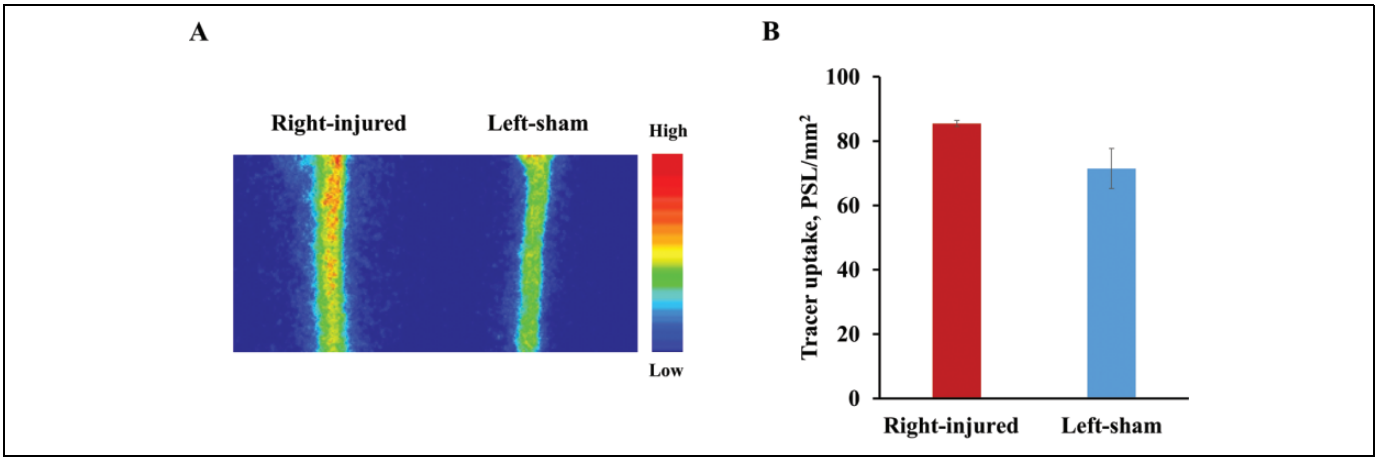

Figure 3. Ex vivo autoradiography of [^{11}C]TZ3321 in balloon injured rat carotid artery. Representative autoradiographic images (A) and the quantification (B, n = 2) confirmed the increased tracer uptake in the injured artery. PSL/mm^2 indicates photostimulated luminescence signals per square millimeter.

bilateral common carotid arteries. The total summary of 1-hour microPET scan images (Figure 1C) indicated higher uptake of [^{11}C]TZ3321 in the right common carotid artery region (the injured side) than in the contralateral artery region (the sham side) at 72 hours postinjury. Tissue time-activity curves of [^{11}C]TZ3321 in bilateral carotid arteries showed a peak at the very first several minutes, which indicated the washout of the radiotracer in the blood and further verified the ROIs that were located in carotid arteries (Figure 2A). Quantification of SUV values revealed statistically higher accumulation of [^{11}C]TZ3321 in the injured carotid artery than in the contralateral artery at 72 hours postinjury. SUV values summed from 15 to 50 minutes of the scan were 0.93 $\pm$ 0.07 and 0.78 $\pm$ 0.09 for the injured and contralateral sides, respectively. The increase percentage was 19.6% (n = 6, P = .001; Figure 2B).

Autoradiographic Studies

Ex vivo autoradiographic data showed modest uptake of [^{11}C]TZ3321 in the sham artery and higher tracer uptake in the injured artery compared to the sham side (Figure 3A). The quantification of the autoradiographic signal of [^{11}C]TZ3321 uptake in the injured artery was 85.5 $\pm$ 0.93 PSL/mm^2, while the value for the contralateral side was 71.48 $\pm$ 6.22 PSL/mm^2 (n = 2, Figure 3B). The increase of the tracer uptake in the injured artery ($\sim$20%) was similar to that measured by SUV values from microPET studies, which further support the quantification method of microPET images.

Histological and Immunological Analysis

The H&E staining showed inflammatory cell infiltration in both intima and adventitia of the injured carotid artery but not

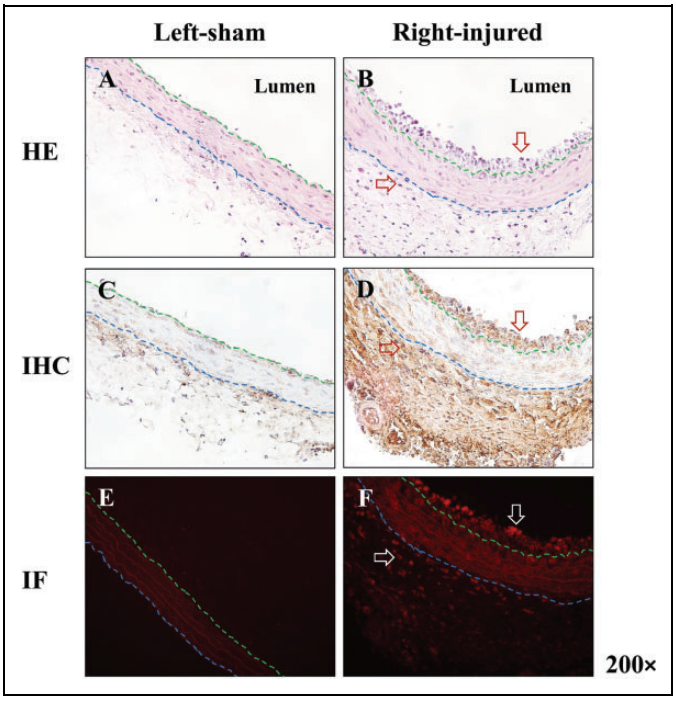

Figure 4. The expression of sphingosine-1-phosphate receptor 1 (S1PR1) in balloon-injured rat carotid artery. A and B, Hematoxylin and eosin (H&E) staining of rat carotid artery (balloon-injured and sham). D and F showed S1PR1 is highly expressed in both intima and adventitia of injured carotid artery. C and E revealed a low level of S1PR1 expression in normal carotid artery. Red/white arrows indicated infiltrated cells (B) or S1PR1-positive cells (D and F). Blue and green dash lines indicated the boundary of intima, media, and adventitia.

in the sham artery (Figure 4). Immunohistochemical staining and immunofluorescence revealed high expression of S1PR1 in these infiltrated cells (Figure 4), which is in agreement with the increased tracer uptake of [^{11}C]TZ3321 in the injured artery. To further explore the cellular colocation of highly expressed S1PR1, antibodies of specific biomarkers of macrophages (CD68), T lymphocytes (CD3), and granulocytes (HIS48) were used for the double immunofluorescence labeling along with S1PR1 antibody. The results showed S1PR1 was expressed on all 3 inflammatory cell types (Figure 5).

Discussion

Inflammation plays an important role in the pathogenesis of many forms of vascular disease, including the response to acute vascular injury.[10] Balloon injury of arteries has been shown to elicit accumulation of leukocytes surrounding the injury site within hours after the insult.[11] The appearance of inflammatory cells is associated with expression of adhesion molecules and leukocyte-specific cytokines, as well as increased S1PR1 level on the injured arteries.[3] Daily intraperitoneal injection of the S1PR1/S1PR3 antagonist VPC44116 (K_i = 30 and 300 nM for S1PR1 and S1PR3, respectively[12]) decreased neointimal hyperplasia by approximately 50%.[3] These data suggest that S1PR1 plays a key role in the pathological changes in response to vascular injury, and it could be a potential target for in vivo monitoring of vascular inflammation by assessing the change of S1P1 expression using PET with a suitable S1P1 radiotracer. In this study, we demonstrated that microPET imaging with a potent S1PR1 radioligand [^{11}C]TZ3321 was able to detect increased S1PR1 expression on the injured carotid artery. In addition, we identified the major contribution of S1PR1 in infiltrated inflammatory cells 72 hours after carotid artery balloon injury.

According to the traditionally considered "inside-out" response, the initial consequences after balloon injury are endothelial denudation and platelet deposition. Circulating leukocytes then bind to the injured surface and migrate across the platelet-fibrin layer and diapedesis into the tissue.[10] There is also an outside-in hypothesis, in which the inflammatory response is orchestrated from the adventitial side of the vessel. Clusters of resident lymphocytes generate local humoral immune responses to produce antibodies against local antigen presentation by foam cells and antigen-presenting cells. The cell populations work in concert to evoke an inflammatory response that propagates inward toward the intima.[13] The histological images from our study detected rapid and obvious infiltration of inflammatory cells in response to balloon injury in both intima and adventitia of the carotid artery, which suggest the "inside-out" and "outside-in" progression may coexist during the early stage of vascular inflammation. More importantly, high S1PR1 expression was observed in these infiltrated cells, which provides a basis for in vivo detection of acute vascular inflammation by PET imaging with a S1PR1-specific radioligand. Concordantly, microPET with the potent and specific S1PR1 radioligand [^{11}C]TZ3321 was utilized in a rat model of carotid artery balloon injury. The tracer uptake in the injured carotid artery was about 19% higher than that in the contralateral intact artery at 72 hours postinjury, which was confirmed by ex vivo autoradiographic study.

We further investigated the cellular location of S1PR1 in the infiltrated cells, including T lymphocytes, macrophages, and granulocytes. S1PR1 is well known for the regulation of lymphocyte migration out of the secondary lymphoid organs into the blood and lymph.[14] FTY-720, a S1PR modulator, was the first Food and Drug Administration–approved oral therapy for multiple sclerosis (MS). The presumed mechanism of action for FTY-720 has been the trapping of autoreactive lymphocytes in the lymphoid organs, away from the central nervous system.[15] Macrophages are important sentinel cells that develop from monocytes to fight infection and repair damaged tissue.[16] The S1PR1 expressed by monocytes and macrophages regulates their migration and recruitment toward S1P.[17] In agreement with that, KRP-203, an S1PR1-specific agonist, blocks S1P signaling through S1P receptor internalization and degradation and downregulates biomarkers for macrophage activation.[18] The S1PR1 was also necessary for the recruitment of neutrophils, which are the first immune cell line of defense and can shape the immune response.[19,20] Specific S1PR1 antagonism blocked neutrophil infiltration, whereas S1PR1 agonism increased sensitivity.[21] The immunofluorescence

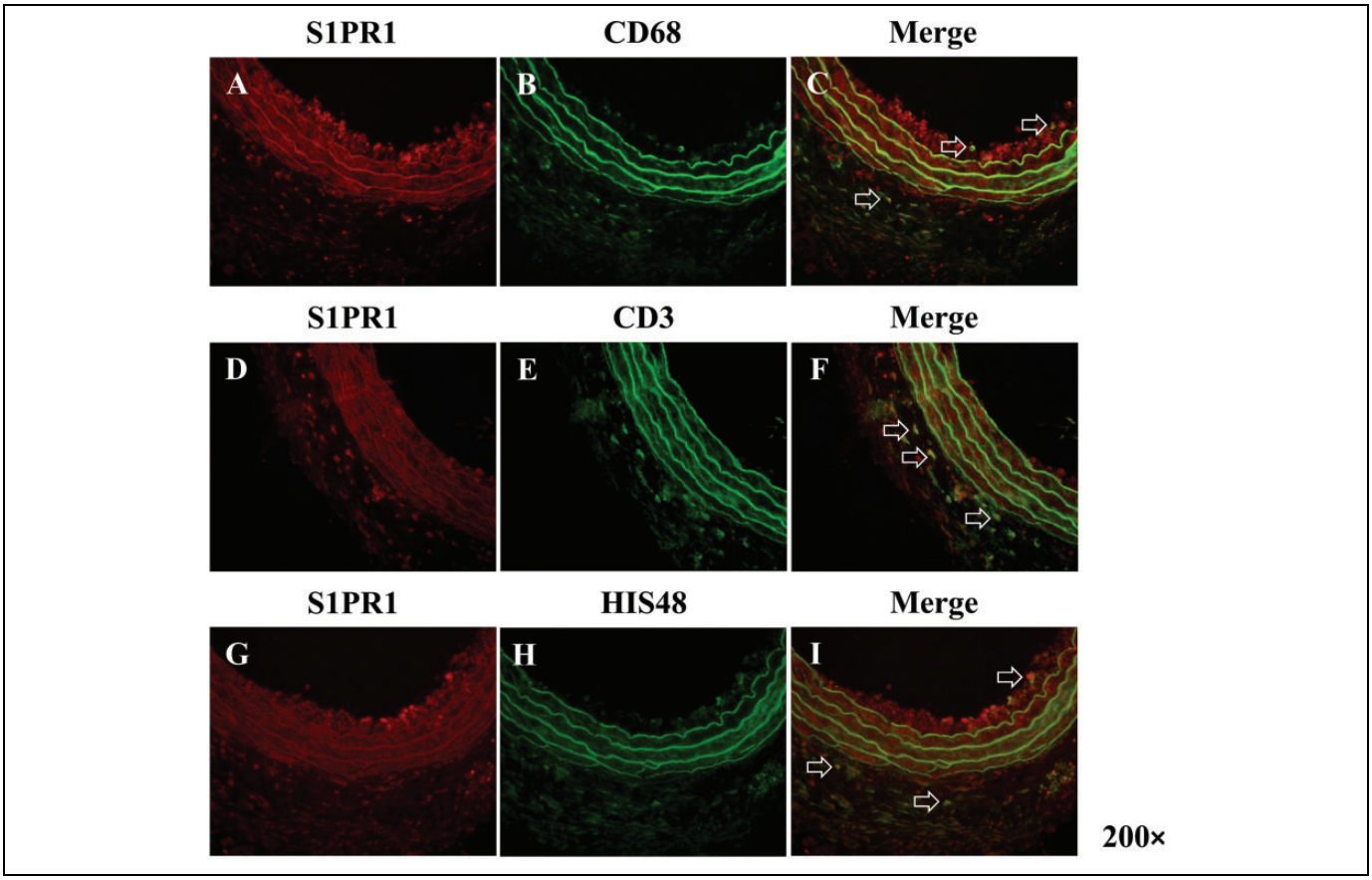

Figure 5. Coregistration of S1PR1 with biomarkers of inflammatory cells in balloon-injured rat carotid artery. A, D, and G, S1PR1 immunofluorescence (red) showed high S1PR1 expression in the injured artery. B, E, and H, CD68/CD3/HIS48 immunofluorescence (green) showed the localization of macrophages, T lymphocytes, and granulocytes in the injured artery, respectively. C, F, and I, coregistration of S1PR1 and CD68/CD3/HIS48 immunofluorescence. White arrows indicated the colocation of S1PR1 in macrophages, T lymphocytes, and granulocytes (yellow).

imaging confirmed S1PR1 expression in these 3 inflammatory cells in the injured site of carotid artery. Therefore, upregulated S1PR1 level in the injured carotid artery is mainly attributed to the infiltration of inflammatory cells that express S1PR1. Accordingly, increased uptake of the S1PR1-specific radioligand [^{11}C]TZ3321 in the injured artery, determined by microPET imaging and ex vivo autoradiography, is correlated with acute inflammatory response following balloon injury. The finding also agrees with our previous report that microPET with [^{11}C]TZ3321 revealed upregulated S1PR1 expression was associated with glial cell activation and immune cell infiltration in lumbar spinal cord in a rat model of MS.[8]

The S1PR1-specific radioligand [^{11}C]TZ3321 has been previously evaluated in a mouse model of vascular injury at relatively late time points (1-4 weeks postinjury). The microPET imaging showed that [^{11}C]TZ3321 was highly accumulated at the injury site, where enhanced S1PR1 level resulted from migrated VSMCs in the neointima.[7] In fact, in the carotid artery balloon injury rats, VSMC migration and proliferation are observed 2 weeks postinjury[6] and contribute to the progression of neointima. Therefore, [^{11}C]TZ3321 has the potential for in vivo imaging of vascular remodeling in a early stage of carotid injury in rats.

Vascular imaging by PET still remains a challenge, especially for preclinical studies in rodents. First, the diameter of rat common carotid artery is close to the spatial resolution of the Inveon microPET scanner ($\sim$1.5 mm full width at half maximum at center of field of view). Second, high tracer uptake in surrounding organs may impact the accuracy of measuring radioactivity in the target vessel. Nevertheless, rat carotid artery injury and mouse femoral artery injury models provide excellent platforms for in vivo tracer validation of [^{11}C]TZ3321, because both vascular injury models not only induce significant increase of S1PR1 expression in the injury site that is detectable by microPET but also avoid the shading of high tracer uptake from major organs. Further investigation on large animals and particularly on humans will facilitate the implementation of [^{11}C]TZ3321 in imaging vascular inflammation by quantitative PET measures of S1PR1 expression.

Conclusion

Increased expression of S1PR1 in infiltrated inflammatory cells in carotid artery 72 hours following balloon injury in rats was detected by microPET imaging using [^{11}C]TZ3321 and confirmed by ex vivo autoradiography and immunohistological

analysis. The data suggest the potential of [^{11}C]TZ3321 as a PET radiotracer for monitoring early inflammatory response and therapeutic efficacy aimed at reducing vascular inflammation.

Acknowledgments

The authors thank Nicole Fettig, Margaret Morris, Amanda Roth, Lori Strong, and Ann Stroncek for their assistance with the microPET imaging studies and Marlene Scott and Bill Coleman in the Elvie L. Taylor Histology Core Facility of Washington University School of Medicine for sample embedding and H&E staining.

Declaration of Conflicting Interests

The author(s) declared no potential conflicts of interest with respect to the research, authorship, and/or publication of this article.

Funding

The author(s) disclosed receipt of the following financial support for the research, authorship, and/or publication of this article: The support resource of this works includes the Department of Energy—(1) DOE-Training in Techniques and Translation: Novel Nuclear Medicine Imaging Agents for Oncology and Neurology (DOE, No. DESC0008432), (2) Interdisciplinary Training in Translational Radiopharmaceutical Development and Nuclear Medicine Research for Oncologic, Neurologic, and Cardiovascular Imaging (DOE, No. DESC0012737), the National Institutes of Health through the National Institute of Neurological Disorders and Stroke (NINDS, R01NS075527), the National Institute of Mental Health (NIMH, No. MH092797), and the Washington University School of Medicine Mallinckrodt Institute of Radiology (MIR) Cyclotron Facility Allotment #14-017.

References

1. Tarkin JM, Joshi FR, Rudd JHF. PET imaging of inflammation in atherosclerosis. *Nat Rev Cardiol*. 2014;11(8):443–457.
2. Daum G, Grabski A, Reidy MA. Sphingosine 1-phosphate: a regulator of arterial lesions. *Arterioscler Throm Vasc Biol*. 2009;29(10):1439–1443.
3. Wamhoff BR, Lynch KR, MacDonald T, Owens GK. Sphingosine-1-phosphate receptor subtypes differentially regulate smooth muscle cell phenotype. *Arterioscler Throm Vasc Biol*. 2008;28(8):1454–1461.
4. Kono M, Tucker AE, Tran J, Bergner JB, Turner EM, Proia RL. Sphingosine-1-phosphate receptor 1 reporter mice reveal receptor activation sites in vivo. *J Clin Invest*. 2014;124(5):2076–2086.
5. Tasaki T, Yamada S, Guo X, et al. Apoptosis signal-regulating kinase 1 deficiency attenuates vascular injury-induced neointimal hyperplasia by suppressing apoptosis in smooth muscle cells. *Am J Pathol*. 2013;182(2):597–609.
6. Holt AW, Tulis DA. Experimental Rat and Mouse Carotid Artery Surgery: Injury & Remodeling Studies. *ISRN Minim Invasive Surg*. 2013;2013. Article ID 167407. doi:10.1155/2013/167407.
7. Jin H, Yang H, Liu H, et al. A promising carbon-11-labeled sphingosine-1-phosphate receptor 1-specific PET tracer for imaging vascular injury [published online February 5, 2016]. *J Nucl Cardiol*. doi:10.1007/s12350-015-0391-1.
8. Liu H, Jin H, Yue X, et al. PET imaging study of S1PR1 expression in a rat model of multiple sclerosis. *Mol Imaging Biol*. 2016;18(5):724–732.
9. Tulis DA. Rat carotid artery balloon injury model. *Methods Mol Med*. 2007;139:1–30.
10. Simon DI. Inflammation and vascular injury: basic discovery to drug development. *Circ J*. 2012;76(8):1811–1818.
11. Xing D, Miller A, Novak L, Rocha R, Chen YF, Oparil S. Estradiol and progestins differentially modulate leukocyte infiltration after vascular injury. *Circulation*. 2004;109(2):234–241.
12. Foss FW, Snyder AH, Davis MD, et al. Synthesis and biological evaluation of gamma-aminophosphonates as potent, subtype-selective sphingosine 1-phosphate receptor agonists and antagonists. *Bioorgan Med Chem*. 2007;15(2):663–677.
13. Maiellaro K, Taylor WR. The role of the adventitia in vascular inflammation. *Cardiovasc Res*. 2007;75(4):640–648.
14. Matloubian M, Lo CG, Cinamon G, et al. Lymphocyte egress from thymus and peripheral lymphoid organs is dependent on S1P receptor 1. *Nature*. 2004;427(6972):355–360.
15. Cohen JA, Chun J. Mechanisms of Fingolimod's efficacy and adverse effects in multiple sclerosis. *Ann Neurol*. 2011;69(5):759–777.
16. Murray PJ, Wynn TA. Protective and pathogenic functions of macrophage subsets. *Nat Rev Immunol*. 2011;11(11):723–737.
17. Cheng Q, Ma S, Lin D, et al. The S1P receptor-selective agonist CYM-5442 reduces the severity of acute GVHD by inhibiting macrophage recruitment. *Cell Mol Immunol*. 2014;12(6):681–691.
18. Poti F, Gualtieri F, Sacchi S, et al. KRP-203, sphingosine 1-phosphate receptor type 1 agonist, ameliorates atherosclerosis in LDL-R-/- mice. *Arterioscler Thromb Vasc Biol*. 2013;33(7):1505–1512.
19. Finley A, Chen Z, Esposito E, Cuzzocrea S, Sabbadini R, Salvemini D. Sphingosine 1-phosphate mediates hyperalgesia via a neutrophil-dependent mechanism. *PLoS One*. 2013;8(1):e55255.
20. Nathan C. Neutrophils and immunity: challenges and opportunities. *Nat Rev Immunol*. 2006;6(3):173–182.
21. Blaho VA, Hla T. An update on the biology of sphingosine 1-phosphate receptors. *J Lipid Res*. 2014;55(8):1596–1608.